Originals

Heat and Mass Transfer 32 (1997) 143–148 © Springer-Verlag 1997

Numerical solutions of pulsating flow and heat transfer characteristics in a channel with a backward-facing step

A. Valencia, L. Hinojosa

Abstract The incompressible laminar flow of air and heat transfer in a channel with a backward-facing step is studied for steady cases and for pulsatile inlet conditions. For steady flows the influence of the inlet velocity profile, the height of the step and the Reynolds number on the reattachment length is investigated. A parabolic entrance profile was used for pulsatile flow. It was found with amplitude of oscillation of one by $Re = 100$ that the primary vortex breakdown through one pulsatile cycle. The wall shear rate in the separation zone varied markedly with pulsatile flows and the wall heat transfer remained relatively constant. The time-average pulsatile heat transfer at the walls was greater as with steady flow with the same mean Reynolds number.

Numerische Lösungen für das Wärmeübergangsverhalten bei pulsierender Strömung in einem Kanal mit stromaufwärts liegender Stufe

Zusammenfassung Es wird eine zweidimensionale numerische Untersuchung des instationären Wärmeübergangs und Druckverlustes im laminar durchströmten Spaltkanal mit einer plötzlichen Kanalerweiterung dargelegt und zwar für stationäre und periodische Geschwindigkeitsprofile am Eintritt des Kanals. Für stationäre Strömungen wurden die Form des Eintrittsprofils, die Reynoldszahl und die Kanalerweiterung variiert. Als Lösung der Navier/Stokes-und der Energiegleichungen mit periodischen Randbedingungen resultiert eine oszillierende Strömung, die das Aufplatzen des Primärwirbels in einer Schwingungsperiode zur Folge hat. Der Einfluß dieser Oszillation auf den Wärmeübergang und den Strömungsverlust wurde für die maximale Amplitude und für $Re = 100$ eingehend untersucht.

Received on 6 March 1996

A. Valencia
L. Hinojosa
Departamento de Ingeniería Mecánica
Universidad de Chile
Casilla 2777, Correo 21
Santiago, Chile

Correspondence to : A. Valencia

Dedicated to Professor Martin Fiebig, Institut für Thermo- und Fluiddynamik, Ruhr-Universität Bochum on his 65 birthday, who trained me and support me in the steps of my career.

The financial support received of CONICYT-CHILE under grant No. 1950559 is gratefully acknowledged.

List of symbols

A	amplitude of oscillation
c	specific heat
C_f	wall friction coefficient
D_H	hydraulic diameter ($=2h$)
E	expansion ratio ($=s/H$)
f	frequency
h	upstream channel height
H	downstream channel height
k	thermal conductivity
l	upstream channel length
L	downstream channel length
Nu	local Nusselt number ($=\alpha(x)2h/k$)
p	pressure
Pr	Prandtl number
Re	Reynolds number
s	step height
St	Strouhal number ($=f2h/U_0$)
t	time
T	temperature
T_0	inlet fluid temperature
T_w	channel wall temperature
T_b	bulk temperature
u	horizontal velocity component
U_0	average velocity at the inlet
v	vertical velocity component
x	horizontal Cartesian coordinate
y	vertical Cartesian coordinate
x_R	first recirculating region length

Greek symbols

$\alpha(x)$	local heat transfer coefficient
θ	dimensionless temperature
μ	dynamic viscosity
ρ	density
τ	dimensionless time
τ_W	wall shear stress

1 Introduction

The flow over a backward-facing step is a classic fluid-mechanics benchmark problem and has been the subject of numerous experiemtnal and numerical studies (e.g. [1–4]). Figure 1 shows a diagram of the flow geometry. Fluid with

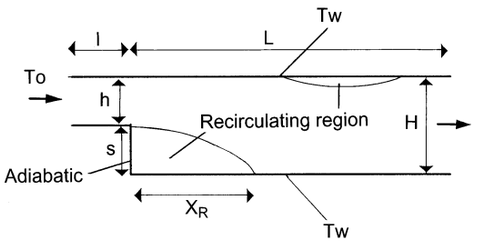

Fig. 1. Schematic diagram of flow domain

constant density ρ and viscosity μ enters the upstream channel of height h with a prescribed velocity profile (uniform or parabolic). After travelling a distance l, the fluid passes over a backward-facing step (discontinuity in channel height) of height s and enters the downstream channel of height $H=h+s$. After travelling a distance L downstream of the step, the fluid exists the region of interest. For Reynolds number considered here, the flow separates at the corner and forms a recirculating region of length X_R behind the step. Additional recirculating regions form on the upper and subsequently the lower walls of the downstream channel as the Reynolds number is increased, Armaly et al. [1].

Two parameters characterize this flow: the Reynolds number based on upstream conditions, $Re=\rho U_0 2h/\mu$, and the channel expansion ratio, $E=s/H$. Although there are additional geometric parameters (l/h and L/h), they are usually assumed to be sufficiently large so that further increases in their values do not change the flow. Demuren et al. [2] demonstrate that numerical solutions are unaffected by increases in L/h beyond a 7. There was no difficulty in obtaining the correct results even though a recirculating eddy was dissected by the outflow boundary for the domain length of 7 by $Re=800$. In accordance with Kaiktsis et al. [3], for $Re>100$, the value of l/h may be set equal to any value between zero and infinity with parabolic entrance velocity profile in numerical simulations without significantly affecting the flow downstream of the step.

One benchmark result often reported in both numerical and experimental investigations is the dependence of X_R/s, the length of the recirculation region downstream of the step normalized by the step height, on the Reynolds number, Re. Kaiktsis et al. [3] present a plot of X_R/s as a function of Re, as determined by a variety of computational and experimental investigations. Agreement is good up to $Re=400$, beyond which point the results of two-dimensional computation begin to fall systematically below the experimental results. Armaly et al. [1] also observed this discrepancy and explained it as resulting from significant three-dimensionality in the experimental flow that arises as soon as the second recirculating region forms on the upper channel wall at $Re\sim400$.

Another quantity more difficult to obtain is the Reynolds number at which the flow first exhibits sustained unsteady behavior. The experiments of Armaly et al. [1] indicate that a significant increase in velocity fluctuations occurs for $Re>1200$, indicating the onset of transition to turbulence. Since their flow is highly three-dimensional at this Reynolds number, it is unclear how this result relates to the onset of sustained unsteady flow in the corresponding two-dimensional simulations of flow over a backward-facing step at the conditions of Armaly. Kaiktsis et al. examine the long-time behavior of the two-dimensional flow and find that the flow is oscillatory at $Re=700$, and fully chaotic at $Re=800$. However, numerical simulation of Torczynski [4] shows that the resolution required to obtain asymptotically steady behavior increase with Reynolds number. This suggests that the reported transition to sustained chaotic flow be an artifact of inadequate spatial resolution.

Thangam et al. [5] find that the reattachment length varied linearly with the step height. Kondoh et al. [6] studied the flow and heat transfer downstream of a backward facing-step and reported that the peak of the local Nusselt number does not necessarily locate at the point of flow reattachment. Hong et al. [7] show the effects of the inclination angle and Prandtl number on the reattachment length and the Nusselt number with laminar mixed convection.

An interesting application is the observation of pulsatile flows in channels with a flow separation (e.g. backward-facing step). The study of the behavior of the flow and heat transfer for these conditions has not been very undertaken in the technical literature. Sobey [8] carried out experimental and numeric tests with both asymmetric and symmetric two-dimensional expansions. The observation of a vortex wave though a right-angled expansion with $Re=80$, and $St=0.003$ shows that the center of the primary vortex was further downstream than in the case of steady flow and a secondary vortex was observed as a consequence of the unsteady nature of the flow. Heat and mass transfer in the sudden expansion region of a pipe under pulsatile conditions was studied by Ma et al. [9], for high Prandtl and Schmidt numbers. They found that the time-average pulsatile heat transfer at the wall was approximately the same as with steady flow with the mean Reynolds number.

The objective of this study consists in a numerical analysis of the flow and heat transfer in a channel with a backward-facing step with steady and pulsatile inlet velocity profile. For stationary flows the influence of the inlet velocity profile, the height of the step and the Reynolds number on the reattachment length is reported. A parabolic entrance profile was used for pulsatile flow. Special attention was paid to how the wall friction and the local heat transfer vary in a situation with amplitude of oscillation of one. The results provide a detailed description of the fluid flow and heat transfer characteristics under the combined influence of flow separation and pulsatility.

2 Mathematical formulation

2.1 Governing equations

The conservation equations describing the flow are the time-dependent, two-dimensional Navier–Stokes equations and the energy equation for a constant property incompressible fluid. They are given here in non-dimensional Conservative form.

Continuity:

$$\frac{\partial U}{\partial X}+\frac{\partial V}{\partial Y}=0 \tag{1}$$

Momentum:

$$\frac{\partial U}{\partial \tau}+\frac{\partial U^2}{\partial X}+\frac{\partial UV}{\partial Y}=-\frac{\partial P}{\partial X}+\frac{1}{Re}\left(\frac{\partial^2 U}{\partial X^2}+\frac{\partial^2 U}{\partial Y^2}\right) \tag{2}$$

$$\frac{\partial V}{\partial \tau}+\frac{\partial UV}{\partial X}+\frac{\partial V^2}{\partial Y}=-\frac{\partial P}{\partial Y}+\frac{1}{Re}\left(\frac{\partial^2 V}{\partial X^2}+\frac{\partial V^2}{\partial Y^2}\right) \tag{3}$$

Energy:

$$\frac{\partial \theta}{\partial \tau}+\frac{\partial U\theta}{\partial X}+\frac{\partial V\theta}{\partial Y}=\frac{1}{Re\,Pr}\left(\frac{\partial^2 \theta}{\partial X^2}+\frac{\partial^2 \theta}{\partial Y^2}\right) \tag{4}$$

where the following dimensionless variables are defined:

$$X=\frac{x}{2h},\quad Y=\frac{y}{2h},\quad \tau=\frac{tU_0}{2h},\quad \theta=\frac{T}{T_0} \tag{5}$$

$$U=\frac{u}{U_0},\quad V=\frac{v}{U_0},\quad P=\frac{p}{\rho U_0^2},\quad Re=\frac{\rho U_0 2h}{\mu},\quad Pr=\frac{\mu c}{k} \tag{6}$$

The lower case letters denote a dimensional variable and the u and v velocity components correspond to the x- and y-directions of the Cartesian coordinate system. The temperature is denote by T and the dynamic pressure by p. The various terms in the equations are nondimensionalized using the fluid density ρ, the hydraulic diameter of the upstream channel $2h$, and U_0, the average velocity upstream of the channel. The time has been normalized with the convective time scale.

2.2
Boundary conditions

For steady flows, both uniform and parabolic inlet velocity profiles are used with $l/h=0$. The fluid is maintained at a constant temperature at the inlet which is lower than that of the wall. The walls are treated as no-slip with a constant temperature $\theta_w=2$. For steady flow at the inlet

uniform: $U=1.0$ and $V=0$

parabolic:

$$Up=3/b^2((Y-E)b-(Y-E)^2/2)$$

with $b=h/2H$, $E=s/H$ is the expansion ratio of the channel, and $V=0$

$\theta=1.0$

For pulsatile flow, the axial velocity component in this study is assumed to be the fully developed velocity profile in a channel and sinusoidal in time.

$U=Up(1+A\sin St\,\tau)$ and $V=0$, $\theta=1.0$

where A is the amplitude of oscillation, and St is the Strouhal number or the nondimensional frequency of oscillation. Initially, for $\tau=0$; $U=Up$, $V=0$ and $\theta=1$ at all locations. At the exit, the boundary conditions for the dependent variables are obtained by setting the first derivatives in the axial direction equal to zero. Although this boundary condition is strictly valid only when the flow is fully developed, its use in other flow conditions is also permissible for computational convenience provided the outlet boundary is located in a region where the flow is in the downstream direction, and sufficiently far downstream from the region of interest, Demuren et al. [2].

The flow configuration for the numerical calculation can be geometrically described by the following non-dimensional parameters for steady flows: length $L/H=10$, $E=0.25$, 0.5, 0.75. The channel Reynolds number was varied from 100 to 1250. For pulsatile flows: $A=0.2$, 0.5, 1.0, $St=1.0$, $E=0.5$, $Re=100$ and $L/H=5.0$. The working fluid is air, $Pr=0.71$, and the direction of the air flow is from left to right.

2.3
Physical parameters

In the presentation of the results two additional dimensionless parameters were involved. The wall shear stress, and heat transfer coefficients were presented in terms of friction coefficient and Nusselt number respectively:

$$C_f=\frac{\tau_W}{1/2\,\rho U_0^2} \tag{7}$$

$$Nu(x)=\frac{\alpha(x)2h}{k}=\frac{(\partial T/\partial y)_{wall}\,2h}{(T_b(x)-T_w)} \tag{8}$$

The bulk temperature was calculated using the velocity and the temperature distribution with the equation:

$$T_b(x)=\frac{\int_0^H uT\,dy}{\int_0^H u\,dy} \tag{9}$$

3
Numerical solution technique

The discretization method used in the present study uses a control volume formulation. The domain of interest is divided into a set of discrete control volumes. A grid point is located at the center of each control volume and the value of the conserved variable is stored at each of the grid points. Discretization equations for the nodal unknown at a grid point are then obtained by conserving the flux of that variable over the control volume that surrounds the grid point. This requires the evaluation of the total flux of the conserved variable through each face of the control volume. In the present study the power-law scheme proposed by Patankar, [10], is used to compute the combined convection and diffusion flux through a control volume face in terms of the values of the variable at the grid points which envelop the face. A staggered grid is employed for storing the velocity components. Thus the control volume for the x-(or y-) direction velocity is displaced in the x-(or y-) direction with respect to the control volume for continuity. This use of a staggered grid prevents the occurrence of checkerboard pressure fileds. A detailed description of this discretization method is given in [10]. Several modifications to the application of SIMPLE method were recommended in [11] including the SIMPLEC approximation, TDMA solver and convergence criterion for the pressure equation. These modifications are employed in the present algorithm. For these computations a 202×22 grid has been used with steady flows ($L/H=10$) and 102×22 with pulsatile flows ($L/H=5$). In order

to study the grid independence, one steady case was run with 302×32 grid points as well for $Re = 200$ and uniform inlet velocity profile. The computation results show a difference of only 4% in the location of reattachment length X_R. Since the computation time with 302×32 grids is nearly eight times that with 202×22 grids, the computation with 302×32 grids is abandoned in favor of 202×22 grids. The time increment between two successive time steps was set as a 0.01. A run of 2000 time steps of size equal to 0.01 units of nondimensional times with pulsatile inlet velocity ($A = 1.0$, $St = 1.0$, $Re = 100$, $E = 0.5$, $L/H = 5.0$), takes about 4000 CPU minutes on an IBM Power PC workstation.

4
Results and discussion

4.1
Steady flows

The results of the backward-facing step flows, especially the reattachment length is sensitive to the numerical procedure used. The adequateness of the present numerical procedure is evaluated by comparing the present predictions of reattachment location with the experimental results of Armaly et al. [1], Fig. 2. Agreement with the experimental results of Armaly et al. is good up to $Re = 500$, beyond which point the results of the two-dimensional computation begin systematically to fall. The discrepancy is explained as resulting from significant three-dimensionality in the flow for $Re > 400$.

In a channel with specified expansion ratio, different inlet velocity profiles result in noticeable differences in the reattachment length, Fig. 2. With uniform inlet velocity profile the wall shear stress at the upper wall is higher as with parabolic velocity profile and so is the reattachment length smaller.

The variation of the reattachment length for Reynolds number ranging from 100–1250 and expansion ratios ranging from 0.25–0.75 are summarized in Fig. 3. The figure also displays the results of Thangam et al. [5]. The results indicate that for a fixed expansion ratio, the increase in reattachment length with the Reynolds number exhibits a moderately nonlinear trend, which is seen to be more pronounced at higher values of the expansion ratios. It should be noted that flows at high expansion ratios, or Reynolds number, can cause the flow to separate along the upper wall, causing an additional downward displacement of the flow, which, in turn, will retard the growth of the primary eddy.

4.2
Pulsatile flow and heat transfer

The time-dependent recirculation regions at time increments of 0.125 of one oscillation period are shown in Fig. 4 for $A = 1.0$, $St = 1.0$, $E = 0.5$, $L/H = 5$, and $Re = 100$, through the

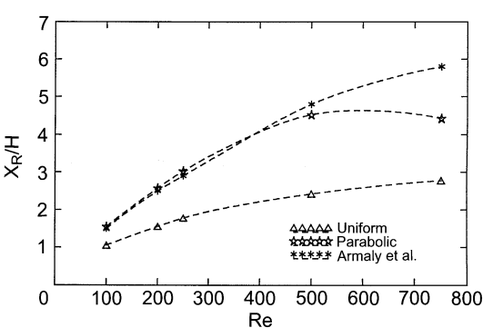

Fig. 2. Recirculation length, X_R, normalized by downstream channel height, H, versus Reynolds number, Re, for parabolic and uniform upstream velocity profile

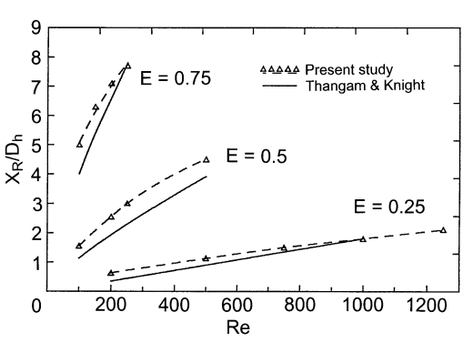

Fig. 3. Variation of the reattachment length with the Reynolds number for different values of expansion ratios. $E = s/H$

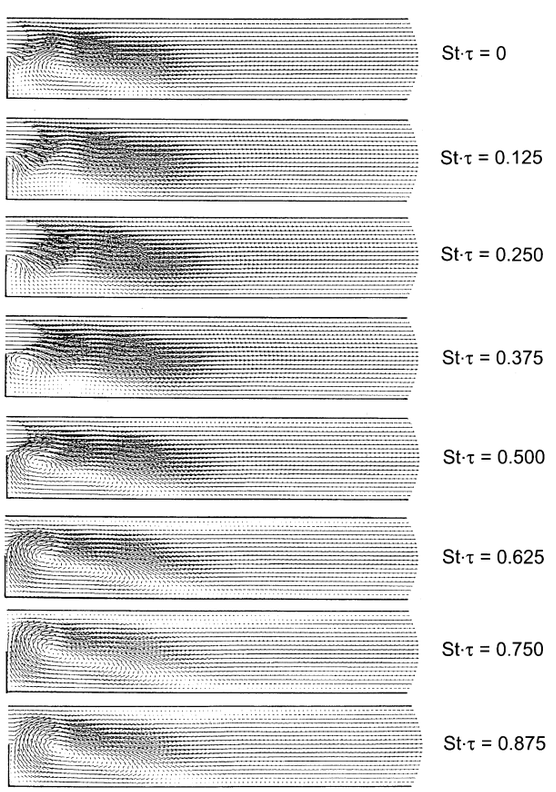

Fig. 4. Temporal sequence of velocity vectors for pulsatile flow at eight selected points for a sinusoidally-varying pulsatile flow with $Re = 100$ and $A = 1.0$. The time increment is 0.125 in each flow pattern

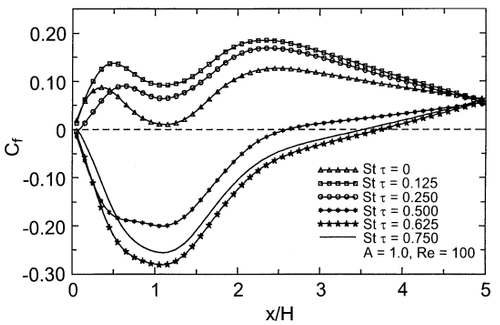

Fig. 5. Variation of the local wall friction factor coefficient at the lower channel wall in one cycle of pulsatile flow

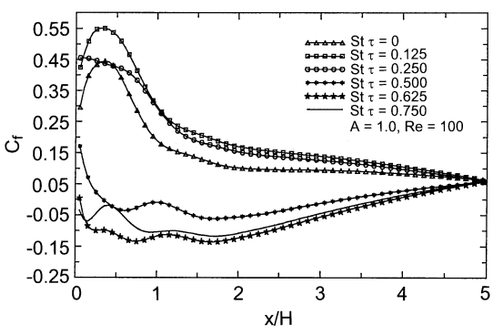

Fig. 6. Variation of the local wall friction factor coefficient at the upper channel wall in one cycle of pulsatile flow

instantaneous computed velocity vectors, when the flow hat reached a periodic steady state after eight cycles. The velocity vectors show considerable variation through the pulsatile cycle. At the onset of the cycle ($St\cdot\tau=0$), the velocity vectors show that the recirculation zone has the same size of steady flow at the same instantaneous *Re*. The recirculation zone breakdown by ($St\cdot\tau=0.125$). The primary vortex born on the corner of the backward-facing step wall at the maximal inlet velocity, instantaneous $Re=200$ ($St\cdot\tau=0.25$), and fill the channel at the minimal inlet velocity, instantaneous $Re=0$, ($St\cdot\tau=0.75$). As the fluid flux was decreased there was a general deceleration of the flow, expressed by an adverse pressure gradient throughout the channel. At this stage was observed the expansion of the vortices in the channel.

The normalized shear stress coefficient variations along the lower wall and upper wall are displayed in Figs. 5 and 6 respectively, at six time instants of the cycle, where C_f is evaluated at the mean Reynold number $Re=100$. The instantaneous wall shear stress distribution varies markedly with time, and the minimum of C_f with decrease of the inlet flow, $St\cdot\tau>0.375$, is higher as the shear stress with steady flow. The minimum wall friction coefficient at the lower wall by steady flow and $Re=100$ is $C_f=0.05$ and with pulsatile flow is $C_f=0.28$ by $St\cdot\tau=0.625$. Figure 5 shows that for $St\cdot\tau<0.375$ the primary vortex does not exist or did not reach the lower wall, $C_f>0$.

Figure 7 shows the variation of the average friction coefficient at the lower channel wall for different amplitude of the pulse as a function of time. The amplitude of the oscillation

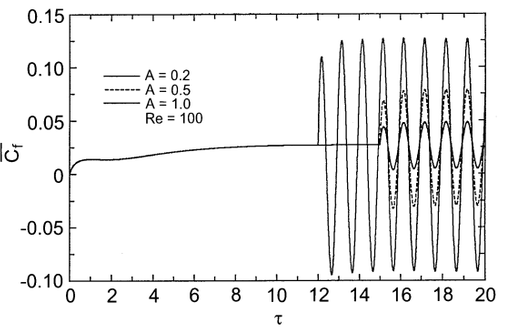

Fig. 7. Average wall friction coefficient at the lower channel wall for different amplitude of the pulse as a function of time

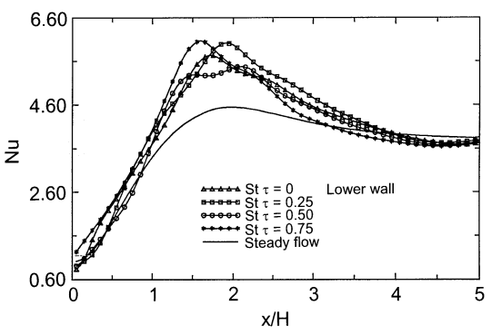

Fig. 8. Local heat transfer coefficient at the lower channel wall at four selected time points in one cycle, $A=1.0$, $Re=100$

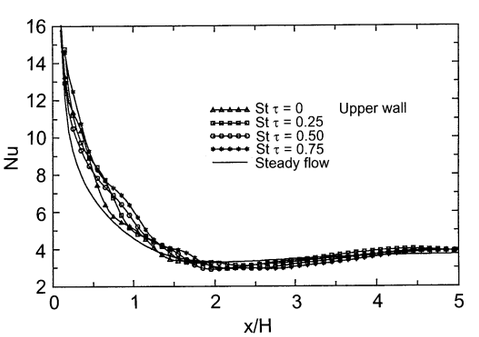

Fig. 9. Local heat transfer coefficients at the upper channel wall at four selected time points in one cycle, $A=1.0$, $Re=100$

of the average friction coefficient varies with the amplitude of the pulse and the friction coefficient can be negative for $A>0.2$.

In contrast, heat transfer on the channel walls change less through one pulsatile cycle. The local heat transfer coefficient variations along the lower and upper walls are displayed in Figs. 8 and Fig. 9 respectively, at four time instants of the cycle. The maximum heat transfer coefficient varies less than 15% over the pulsatile cycle on the lower wall and was only 35% greater in magnitude in comparison with steady flow at the mean Reynolds number, see Fig. 8. The variation of the local heat transfer on the upper channel through the pulsatile cycle is small, see Fig. 9.

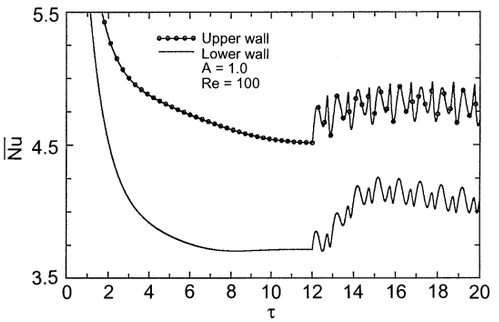

Fig. 10. Average Nusselt number at the upper and lower channel walls as a function of time

The relationships among the locations of zero shear stresses and maximum heat transfer coefficient on the lower channel wall during one cycle is not clear as with steady flows. The flow parameter of the reattachment point, $C_f = 0$, move widely, $0 < X_R/H < 3.7$, see Fig. 5, whereas the maximum heat transfer coefficient location shifts only within a narrow range, see Fig. 8. In general the maximum heat transfer at the lower wall during pulsatile flow is located close to the point seen with steady flows at the mean Reynolds number.

The variation of the average heat transfer coefficient at the lower and upper channel walls with the time show Fig. 10. The average heat transfer enhancement on the lower channel wall is about 9%. The average heat transfer coefficient variation is not sinusoidal in time as the inlet velocity profile.

Understanding of wall shear stress and heat transfer in separated regions has important implications to practical flows. Heat transfer was examined here in the recirculation region behind a backward-facing step as function of the amplitude of the pulsatile flow. The pulsatility of the flow did not appear to impact the heat transfer in separated region as the wall shear stress.

5 Conclusions

The laminar flow and heat transfer phenomena were studied in a channel with a backward-facing step under steady and pulsatile conditions. The Reynolds number was varied from 100–1250, the expansion ratio from 0.25–0.75 and the entrance velocity profile was also varied for steady flow. It was found that heat transfer in the lower wall was maximal downstream the reattachment length for steady flows.

In one cycle with pulsating flow ($A = 1.0$, $St = 1.0$, $E = 0.5$, $L/H = 5.0$, $Re = 100$, $Pr = 0.71$) and parabolic inlet velocity profile, breakdown of the primary recirculation zone was observed. The primary vortex born on the corner of the backward-facing step wall at the maximal inlet velocity ($St \cdot \tau = 0.25$), and fill the channel at the minimal inlet velocity ($St \cdot \tau = 0.75$). The friction coefficient is negative and positive through one cycle.

Pulsating flow caused the movement of maximum heat transfer on the lower wall in the cycle. The time-average pulsatile heat transfer at the channel walls was approximately only 9% higher as with steady flow with the mean Reynolds number by $Re = 100$ and $A = 1.0$.

References

1. **Armaly, B.F.; Durst, F.; Pereira, J.C.F.; Schönung, B.:** Experimental and theoretical investigation of backward-facing step flow. J. Fluid Mech. 127 (1983) 473–496.
2. **Demuren, A.; Wilson, R.:** Estimating uncertainty in computations of two-dimensional separated flows. J. Fluids Eng. 116 (1994) 216–220
3. **Kaiktsis, L.; Karniadakis, G.E.; Orszag, S.A.:** Onset of three dimensionality, equilibria and early transition in flow over a backward-facing step. J. Fluid Mech. 231 (1991) 501–528
4. **Torczynski, J.R.:** A grid refinement study of two-dimensional transient flow over a backward-facing step using spectral-element method. In: Separated Flows, FED-Vol 149. American Society of Mechanical Engineers, New York, (1993) 1–7
5. **Thangam, S.; Knight, D.D.:** Effect of step height on the separated flow past to backward facing step. Phys. Fluids A 1 (1989) 604–606
6. **Kondoh, T.; Nagano, Y.; Tsuji, T.:** Computational study of laminar heat transfer downstream of backward-facing step. Int. J. Heat Mass Transfer 36(3) (1993) 5577–591
7. **Hong, B.; Armaly, B.F.; Chen, T.S.:** Laminar mixed convection in a duct with a backward-facing step: the effects of inclination angle and Prandtl number. Int. J. Heat Mass Transfer (12) (1993) 3059–3067
8. **Sobey, I.:** Observation of waves during oscillatory channel flow. J. Fluids Mechanics 151 (1985) 395–426
9. **Ma, P.; Li, X.; Ku, D.N.:** Heat and mass transfer in a separated flow region for high Prandtl and Schmidt numbers under pulsatile conditions. Int. J. Heat Mass Transfer. 37(17) (1994) 2723–2736
10. **Patankar, S.V.:** Numerical Heat Transfer and Fluid Flow. Hemisphere, Washington, DC (1980)
11. **Doormaal, J.P. van; Raithby, G.D.:** Enhancements of the SIMPLE Method for Predicting Incompressible Flow Flows. Num. Heat Transfer 7 (1984) 147–163